Crystalline domain size and faulting in the new NIST SRM 1979 zinc oxide

J. P. Cline[1], M. Leoni[3], D. Black[1], A. Henins[1], J. E. Bonevich[1],
P. S. Whitfield[2], and P. Scardi[3]

[1] National Institute of Standards and Technology, Gaithersburg, MD
[2] National Research Council, Ottawa, Canada
[3] Dept. of Civil, Environmental and Mechanical Engineering, University of Trento, Trento, Italy

A NIST SRM certified to address the issue of crystallite size measurement through a line profile analysis has been under development for several years. In order to prepare the feedstock for the SRM, nano-crystalline zinc oxide was produced from thermal decomposition of zinc oxalate. The thermal processing parameters were chosen to yield particles in two size ranges, one with a distribution centered at approximately 15 nm and another centered at 60 nm. Certification data were collected on a NIST-built diffractometer equipped with a Johansson incident beam monochromator and scintillation detector. Data were analyzed using whole powder pattern modeling to determine microstructural data. The analysis shows domains to be in the form of discs of a fairly small aspect ratio. While both materials exhibit the effects of stacking faults through broadening of specific hkl reflections, their presence in the 60 nm is more difficult to discern. Images of the crystallites obtained with transmission electron microscopy are consistent with the results from the X-ray diffraction analyses.

Key words: NIST, SRM 1979, Line Profile Analysis

INTRODUCTION

The ability to use line profile analysis (LPA) to characterize the crystallite size of a wide range of nano-scale materials is one of the many attributes of modern powder diffraction. The use of LPA has been extensive, as has the research effort into the interpretation of results obtained from various strategies employed in its use. One way to assess performance of a complete measurement method is to acquire and analyze data from a standard sample with known properties. Toward this end the National Institute of Standards and Technology (NIST) developed Standard Reference Material (SRM) 1979, a crystallite size standard. It is based on a

 0885-7156/2013/28(S2)/S2/1/$18.00

nano-scale powder where the crystallites are single diffracting domains and to the largest extent possible, the particles are single grains. The SRM artifact is composed of two individual samples of ZnO powder. One, with a size distribution centered at a crystallite size of 15 nm in diameter, the other with a size distribution centered at a crystallite size of 60 nm in diameter; referred to hereafter as the "15 nm" and "60 nm" materials.

Generally speaking, the diffraction experiment is an inverse problem; the desired outcome is an understanding of a three dimensional structure, although the observation consists only of a one dimensional data set. There are multiple structures, or solutions, which would yield diffraction data corresponding to the observation; the object, of course, is to determine the correct one. The observation of a diffraction experiment is itself a complex object resulting not just from the superposition but also from the convolution of several contributions due to instrument and specimen. In particular, the geometric profile is the convolution of aberration functions resulting from the optics of the instrumentation. The emission spectrum consists of the shape and position, with respect to energy, of the emission profile of the radiation used. The convolution of these two contributions constitutes the instrument profile function (IPF). This is, in turn, convoluted with the specimen broadening function to yield the observation. With whole powder pattern modeling (WPPM) (Scardi & Leoni, 2002), the character of the specimen broadening function is analyzed using functions that explicitly correlate the observation to the microstructural character of the specimen: the result is the set of parameters for the chosen models that are able to best interpret the observation. The term "microstructure" is here employed in a broad sense and includes all specimen-related features that interrupt the regular periodicity of the lattice. The ability to use NIST SRMs for characterization of the IPF has been available since 1989 through the SRM 660(x), LaB_6, series of standards. No standard, however, has been previously available to quantitatively assess microstructural features via powder diffraction.

An "idealized" material for a crystallite size standard would offer a unique character specific to its function as a powder diffraction standard. The desired characteristics include: 1) environmentally stable and non-toxic, 2) exhibiting a strong diffraction signal with "non-overlapped" lines, 3) consist of crystallites of a specific, controllable size range with a narrow size distribution, 4) embody a minimum of crystallographic defects, 5) be dispersible for analysis by complimentary techniques such as transmission electron microscopy (TEM) and 6) be producible in kilogram quantities for SRM production.

https://doi.org/10.1017/S0885715613001188 Published online by Cambridge University Press

Based on an extensive body of earlier work by Louër and Langford (Louër *et al.* (1983), Langford *et al.* (1993), Guillou *et al.* (1995)), an extensive study was pursued to develop a suitable feedstock for SRM 1979. ZnO obtained from the decomposition of zinc oxalate was identified as a viable candidate material. The SRM 1979 feedstock was therefore produced by scaling up the corresponding laboratory procedure to yield a uniform powder in the kilogram quantity needed.

Some features of this new standard are here shown, analyzed and discussed; preliminary results are presented.

EXPERIMENTAL

Following preliminary work on the experimental quantities, a large scale vacuum furnace, capable of decomposing 125 g lots of material at a time, was commissioned. This device can uniformly heat a large powder bed of material, under vacuum, with temperature control precise to ± 0.25 °C, through the 50 °C to 500 °C region. The zinc oxalate precursor powder, 99.999% pure (metals basis), was obtained from Alfa Aesar[1] (Ward Hill, MA). The time/temperature profile of Langford *et al*. (1993) was largely duplicated for the production of the feedstock. The material was heated in the vacuum furnace, rapidly (≈ 6 °C/min) from room temperature to 70 °C, then from 70 °C to 110 °C at a rate of 2 °C/h followed by another rapid increase to 250 °C and then up to 400 °C at 2 °C/h followed by cooling to room temperature. Material was then loaded into a conventional furnace, with no atmospheric control, which was rapidly heated to a temperature of 350 °C and for the 15 nm crystallite size, heated at a rate of 2 °C/h to a final temperature of 400 °C, while for the 60 nm crystallite size the same ramp was used to reach the final temperature of 550 °C. Samples were immediately removed from this second furnace once the final temperature was reached.

The X-ray data used for the certification of SRM 1979 were collected on a NIST-built diffractometer equipped with a Johansson Ge 111 incident beam monochromator, sample spinner and scintillation detector using Cu$K\alpha_1$ radiation. The machine was configured with a 0.8°

[1]Certain commercial equipment, instruments, or materials are identified in this in order to adequately specify the experimental procedure. Such identification does not imply recommendation or endorsement by the National Institute of Standards and Technology, nor does it imply that the materials or equipment identified are necessarily the best available for the purpose.

https://doi.org/10.1017/S0885715613001188 Published online by Cambridge University Press

incident beam slit, 0.05° receiving slit and 4.4° receiving Soller slit. SRM 660b (NIST, 2010) was used to characterize the IPF of the machine. Data were collected in 24 discrete regions straddling the maxima of each profile with the step and scan width of each region being varied in correspondence with the full-width-at-half-maximum of the profiles (FWHM). Count times were varied so as to obtain an approximately constant total number of counts for each scan region. Total data collection time was approximately four days; the data offered 12 – 14 steps over the FWHM. Data from the ZnO specimens were collected in continuous scans from 25° to 125° 2θ with a step width of 0.02° and a count time of 16 s to yield a total scan time of approximately 24 hours. The step width for the "15 nm" sample was increased to 0.025° with a count time of 20 s. An example of these data, with the illustrated IPF profiles, is shown in figure 1.

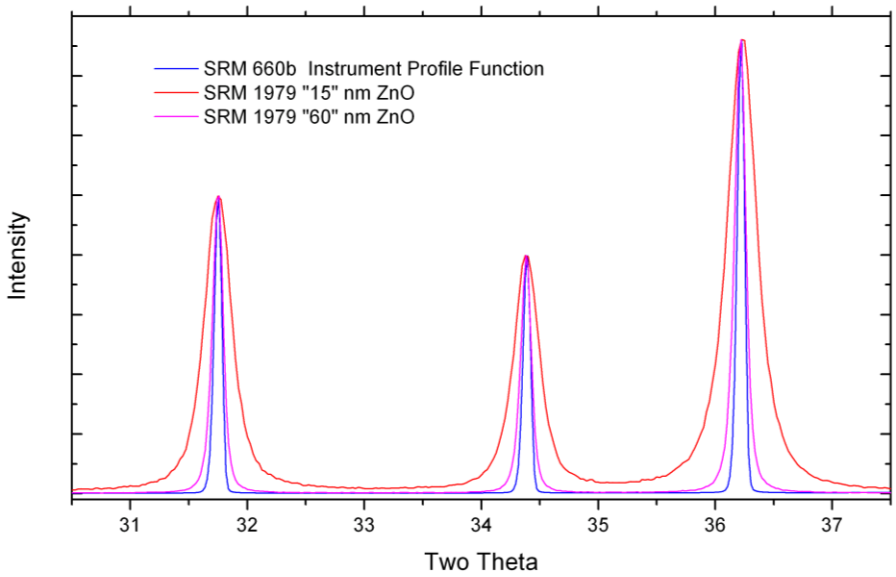

Figure 1. Profiles from SRM 660b, the IPF, and SRM 1979.

Experimental quantities of ZnO, used to test the furnace and develop the annealing schedule, as well test specimens extracted from the individual batches of the final feedstock, were evaluated with a Williamson-Hall (WH) analysis to obtain values for the volume weighted crystallite size, D_V. Data for these analyses were collected on the Siemens D500 diffractometer configured and operated much the same as the aforementioned NIST-built machine. WH plots, from ex-oxalate ZnO samples heated to 400 °C and 550 °C, are shown in figure 2.

https://doi.org/10.1017/S0885715613001188 Published online by Cambridge University Press

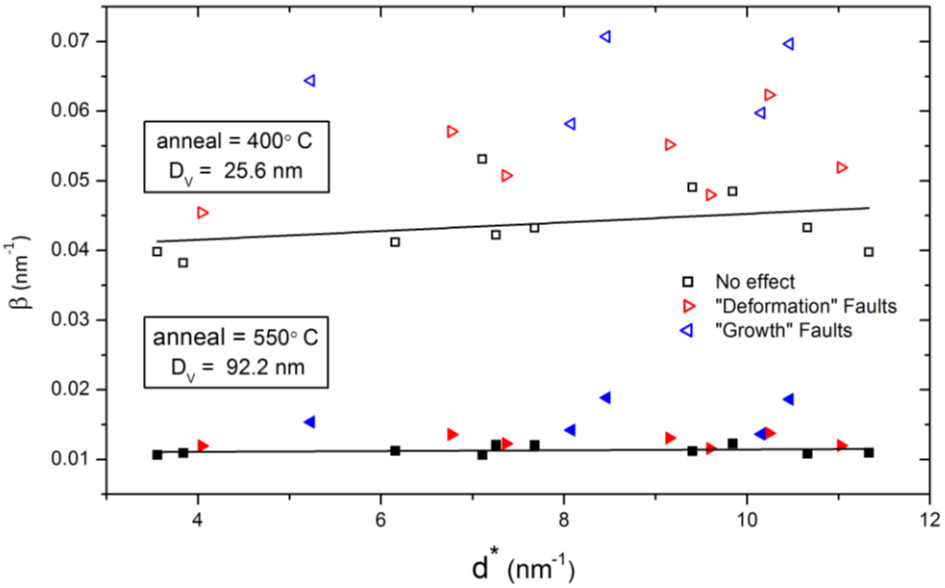

Figure 2. Williamson-Hall plot of ex-oxalate ZnO exhibiting the effects of stacking faults.

The microstructure of the ZnO specimens were analyzed with the WPPM method as implemented in the program PM2K (Leoni *et al.*, 2006). The IPF was modeled within PM2K with 4 pseudo-Voigts for the emission spectrum, three for the $K\alpha_{11}$ and a fourth for the $K\alpha_{12}$. The breadth, intensity and relative contribution of the Lorentzian and Gaussian components of the $K\alpha_{11}$ and $K\alpha_{12}$ lines of the emission spectrum were refined, except the intensity of the first $K\alpha_{11}$ line which was fixed at unity. The positions of the lines, however, were fixed at values reported by Hölzer *et al*. (1997). The U, V, and W parameters of the Caglioti function (Caglioti *et al*., 1958) were refined to model for the FWHM dependence on two-theta and the Finger-Cox-Jephcoat (Finger *et al*., 1994) model was used to account for profile asymmetry due to axial divergence. Lattice parameters were fixed at the certified values; however, the effects of specimen displacement were modeled. The specimen broadening function used was specific to modeling of cylinders of constant aspect ratio with a distribution of diameters presumed to be log-normal. A numerical approach, based on the model for cylinders proposed by Langford & Louër (1982) and the distribution treatment of Scardi & Leoni (2001) and Leoni & Scardi (2004), was employed to calculate the profile for the distributed domains. The Warren (1969) model for hexagonal stacking faults was used. Two parameters can be refined to model the anisotropic peak broadening; the α parameter is proportional to the density of deformation faults, while the β parameter indicates the density of growth faults. This model is strictly valid for stacking faults in an *hcp* ($P6_3/mmc$) ABAB structure (leading to a local *fcc* ABCABC stacking

https://doi.org/10.1017/S0885715613001188 Published online by Cambridge University Press

sequence). Zinc oxide, however, crystallizes in the $P6_3mc$ space group with a wurzite structure, locally changed into sphalerite by the faults. The $P6_3mc$ structure shows an aAbB type of stacking: the phase relationships leading to the recurrence formulae of Warren are analogous to those of the *hcp-fcc* case and therefore the same selection rules and formalism can be employed here.

With the bottling of the bulk feedstock, ten samples were extracted from the population in a stratified random manner for certification measurements. In order to assess the homogeneity of the SRM feedstock, two samples from each bottle were analyzed, for a total of twenty data sets from each of the two powders. Analysis of the 15 nm material with PM2K was straightforward assuming cylindrical domains. Both the aspect ratio and the lognormal mean and variance were refined. It proved problematic to realize convergence with refinements of the coarser, 60 nm ZnO. The strategy that proved successful was to refine that microstructure using a spherical model and then, when convergence was reached, use the cylindrical model. Cumulative size distributions are shown in figures 3 and 4. Fit quality is shown in figures 5 and 6.

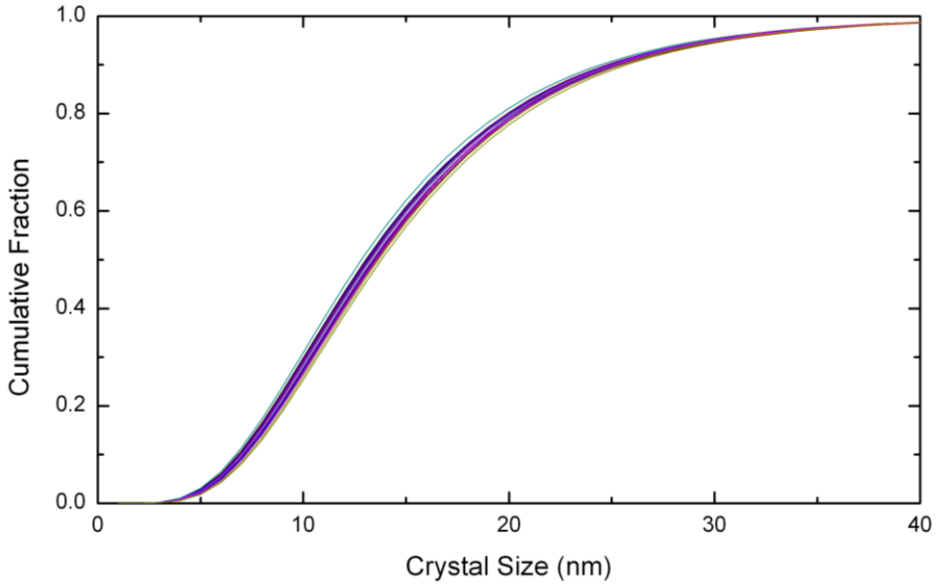

Figure 3. Cumulative size distributions of the 15 nm ZnO obtained with PM2K.

https://doi.org/10.1017/S0885715613001188 Published online by Cambridge University Press

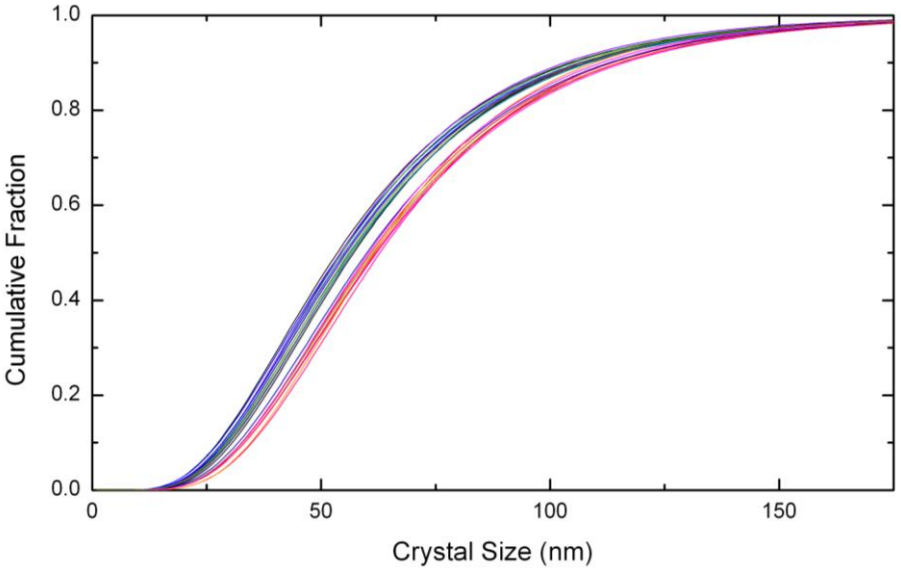

Figure 4. Cumulative size distributions of the 60 nm ZnO obtained with PM2K.

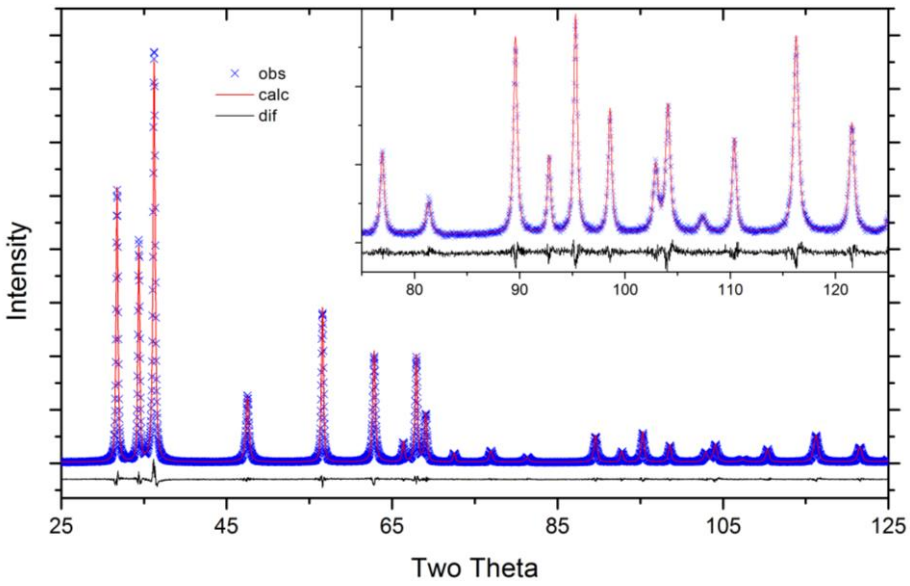

Figure 5. Fit quality obtained using PM2K for analysis of 15 nm ZnO.

https://doi.org/10.1017/S0885715613001188 Published online by Cambridge University Press

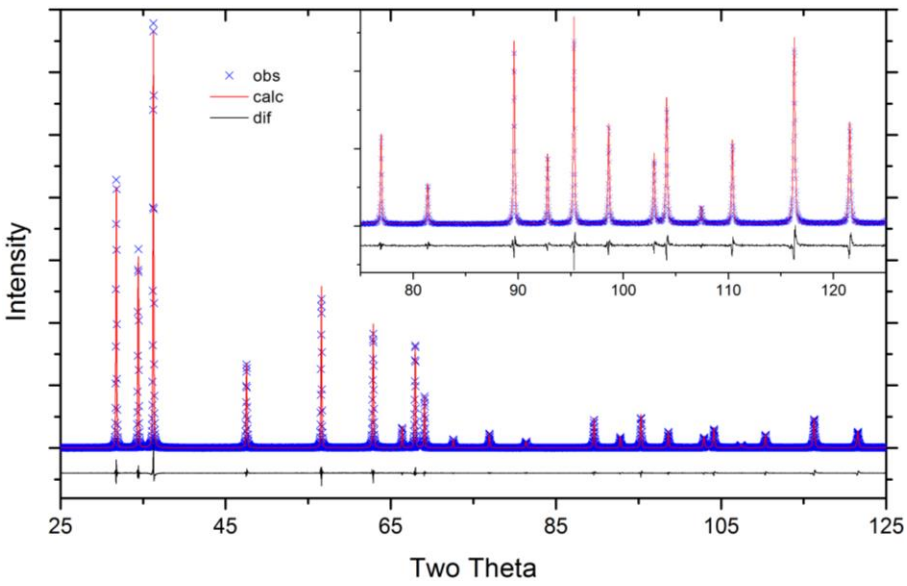

Figure 6. Fit quality obtained using PM2K for analysis of 60 nm ZnO.

RESULTS AND DISCUSSION

The WH plot of figure 2 indicates the presence of stacking faults in the ZnO as observed by Langford *et al.* (1993). Identical trends in the anisotropic broadening with respect to *hkl*, are apparent in both specimens, however; the impact of the stacking faults is markedly reduced at the higher annealing temperature. The peaks can be segregated into three groups; group 1 containing peaks with $h - k = 3n$ exhibiting no broadening effect; group 2 with $h - k = 3n \pm 1$, l odd, that exhibit deformation or strain broadening; and finally group 3 with $h - k = 3n \pm 1$, l even, these exhibit broadening due to growth faults (Auffrédic *et al.*, 1995 and Warren, 1969). The y intercepts of linear fits to the peaks in group 1 of the two samples yielded D_V values of 25.6 nm and 92.2 nm. The slope of a linear fit to the peaks in group 1 of the sample annealed at 400 °C is about 5×10^{-4}, indicating negligible strain. The data of figure 2 were analyzed in the context of the cylindrical shape model as proposed by Langford and Louër (1982) to yield the volume weighted crystallite dimensions. This analysis indicated, for the 400 °C data, a diameter of 26.7 nm and a height of 24.7 nm, for the 550 °C data, the dimensions were a diameter of 108.6 nm and a height of 87.5 nm. These results are consistent with the crystallites being in the form of discs with a fairly small aspect ratio.

https://doi.org/10.1017/S0885715613001188 Published online by Cambridge University Press

The fit quality for the analyses of the two ZnO powders with PM2K was characterized by GoF values - averaged over the 20 analyses - of 1.3 for the 15 nm and 1.5 for the 60 nm indicating that the models used did indeed yield results corresponding to the observation. The mean of the log-normal distributions of diameters for the 15 nm powder was 13.3 nm, with log-normal parameters of $\mu = 2.6$ nm and $\sigma = 0.49$; for the 60 nm material the corresponding values were 58.7 nm, with $\mu = 4.06$ nm and $\sigma = 0.50$. These analyses also indicated that the crystallites were in the form of discs with aspect ratios of 1.12 for the 15 nm ZnO, and 1.29 for the 60 nm material. The Warren model for stacking faults yielded an average β value of 0.011 and vanishingly small α values for the 15 nm material. With the 60 nm material, β values of 0.002 were obtained, with a negligible impact on the residual error terms; the stacking fault model was not used with these analyses. We note the rather large discrepancy between the results from the WPPM analysis and the traditional line profile analysis methods that yield a value for the volume weighted crystallite size.

One observes, from figures 3 and 4, that the range of distributions obtained for the finer material is much narrower than for the coarse one. This is indicative of the increased difficulty of the analysis as the crystallites coarsen and the level of broadening approaches the IPF (cf. figure 1 wherein the 60 nm profiles are surprisingly close to the IPF). Furthermore, careful inspection of the cumulative size distributions of the 60 nm material shown in figure 4 indicates a possible bimodal nature to the data; this observation warrants additional examination. The difficulty in the convergence of the models, observed for the 60 nm powder, can be a possible key to interpret this result.

As a complementary evaluation of the size and shape of the particles, transmission electron microscopy was used. Typical TEM images are shown in figure 7. As can be seen, the particles are prismatic as expected and, where the electron beam could be isolated to a single particle, the diffraction pattern is clearly that from a single-crystal. The smaller material remains aggregated, with the crystallites within the aggregates displaying a noteworthy texture, while the larger material is somewhat irregular in shape. The texture observed in the 15 nm material is consistent with the precursor crystals being quite large, and then decomposing into the smaller oxide crystals with the thermal processing. The presence of stacking faults is clear in the 15 nm material, thus validating the XRD observation.

https://doi.org/10.1017/S0885715613001188 Published online by Cambridge University Press

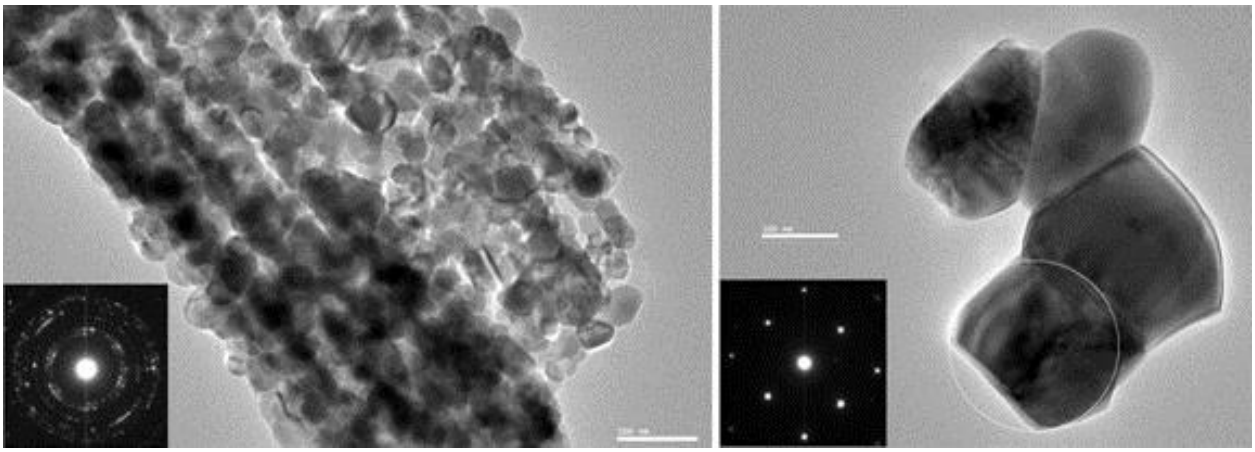

Figure 7**.** TEM images of 15 nm (left) and 60 nm (right) material. The micron marker in both images designates 100 nm.

CONCLUSIONS

Nano-scale crystallites of zinc oxide have been produced by thermal decomposition of a zinc oxalate precursor. The crystallite size is well controlled by proper selection of the processing parameters and the resulting material, while displaying the effects of stacking faults, provides several *hkl* reflections of essentially strain-free single crystal grains. This material will be used for a NIST SRM addressing the issue of domain size measurement from X-ray line profile broadening. The impact of the standard will include the increased use and accuracy of domain size measurements with the powder diffraction method.

ACKNOWLEDGMENT

We would like to thank Dr. Katherine Mullen for her assistance in developing the software used to implement the Langford and Louër (1982) model for integral breadth analysis to yield the crystallite diameter and height.

Auffrédic, J. P., Boultif, A., Langford, J. I. and Louër, D. (**1995**). "Early Stages of Crystallite Growth of ZnO Obtained from an Oxalate Precursor," J. Am. Ceram. Soc. **78**, 323-328.

Caglioti, G., Paoletti, A. and Ricci, F. P. (**1958**). "Choice of Collimators for a Crystal Spectrometer for Neutron Diffraction," Nucl. Instrum. **3**(4), 223-228.

Finger, L.W., Cox, D.E. and Jephcoat, A. P. (**1994**). "A Correction for Powder Diffraction Peak Asymmetry due to Axial Divergence," J. Appl. Crystallogr. **27**, pp. 892–900.

https://doi.org/10.1017/S0885715613001188 Published online by Cambridge University Press

Guillou, N., Auffrédic, J. P. and Louër, D. (**1995**). "The early stages of crystallite growth of CeO_2 obtained from a cerium oxide nitrate," Powder Diffr. **10**, 236-240.

Hölzer, G., Fritsch, M., Deutsch, M., Härtwig, J. and Förster, E. (**1997**). "$K\alpha_{1,2}$ and $K\alpha_{1,3}$ x-ray emission lines of the 3d transition metals," Phys. Rev. A: At., Mol., Opt. Phys. **56**, 4554–4568.

Langford, J. I., Boultif, A., Auffrédic, J. P. and Louër, D. (**1993**). "The use of pattern decomposition to study the combined X-ray diffraction effects of crystallite size and stacking faults in ex-oxalate zinc oxide," J. Appl. Crystallogr. **26**, 22-33.

Langford, J. I. and Louër, D. (**1982**). "Diffraction line profiles and Scherrer constants for materials with cylindrical crystallites," J. Appl. Crystallogr. **15** (1), 20-26.

Leoni, M., Confente, T. and Scardi, P. (**2006**). "PM2K: a flexible program implementing Whole Powder Pattern Modelling," Z. Kristallogr. Suppl. 2006, Issue suppl **23**, 249-254.

Leoni, M. and Scardi, P. (**2004**). "Nanocrystalline domain size distributions from powder diffraction data," J. Appl. Crystallogr. **37**(4), 629–634.

Louër, D., Auffrédic, J. P., Langford, J. I., Ciosmak, D. and Niepce, J. C. (**1983**). "A precise determination of the shape, size and distribution of size of crystallites in zinc oxide by X-ray diffraction line-broadening analysis," J. Appl. Crystallogr. **16**, 183-191.

NIST (**2010**). Lanthanum Hexaboride Powder Line Position and Line Shape Standard for Powder Diffraction (SRM 660b), Gaithersburg, MD; National Institute of Standards and Technology; U.S. Department of Commerce.

Scardi, P. and Leoni, M. (**2001**). "Diffraction line profiles from polydisperse crystalline systems," Acta Crystallogr, Sect. A: Found. Crystallogr. **57** (5), 604–613.

Scardi, P. and Leoni, M. (**2002**). "Whole powder pattern modeling," Acta Crystallogr ., Sect. A: Found. Crystallogr. **58**, 190-200.

Warren, B. E., (**1969**). *X-ray Diffraction* (Dover Publications, Inc., N.Y).

https://doi.org/10.1017/S0885715613001188 Published online by Cambridge University Press